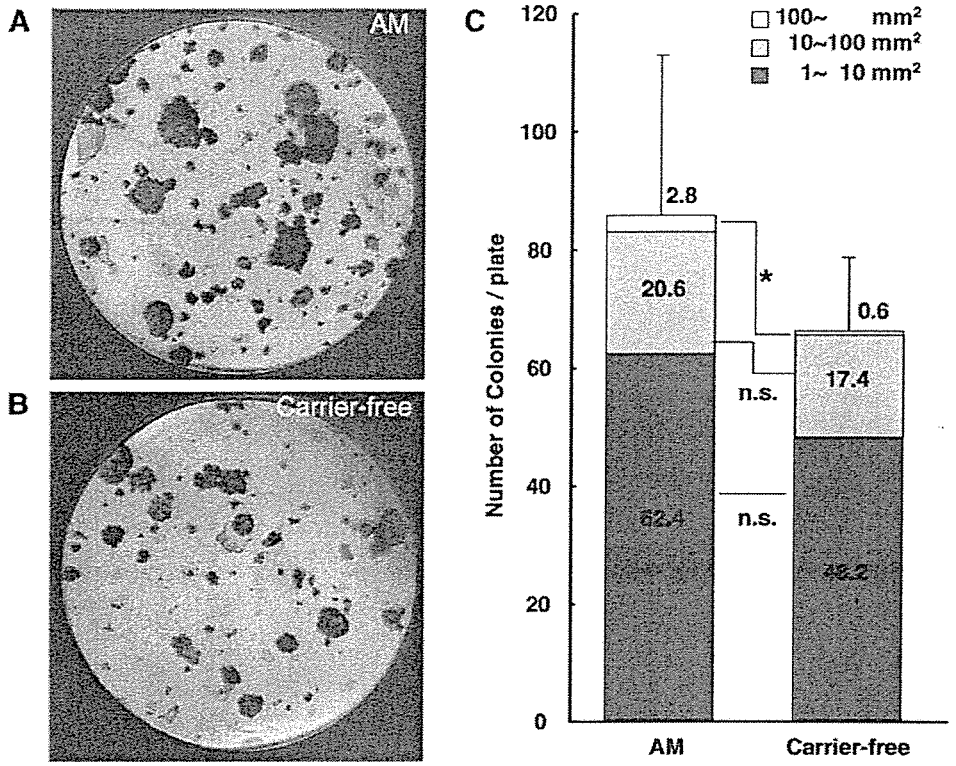

FIGURE 5. Colony formation by disassembled cells. Colony formation by epithelial cells dissociated from AM (A) and carrier-free (B) sheets. Colonies were stained with rhodamine B after 2 weeks. (C) Quantification of size and number of colonies obtained from epithelial sheets ($n = 5$, mean ± SD). There was no significant difference in total colony formation. When cultures were compared by the area of each colony, a significant difference was observed only in the largest colony size ($^*P = 0.014$; Student's t-test, $n = 5$).

mined by a protein assay (DC assay; Bio-Rad Laboratory, Hercules, CA). All samples were then diluted in 2× sample buffer (100 mM Tris-HCl [pH 6.8]), 4% SDS (Invitrogen, Carlsbad, CA), 20% glycerol (Wako), 12% 2-mercaptoethanol (Wako), and boiled. Ten micrograms of each sample were loaded on a 10% Bis-Tris gel (Novex NuPAGE; Invitrogen) and transferred onto polyvinylidene difluoride (PVDF) membranes (Millipore, Billerica, MA). The membranes were blocked with 5% skim milk (Difco Laboratories, Detroit, MI), 1.5% normal goat serum, and PBS for 60 minutes at RT. The membranes were reacted with K3 (AE5) and β-actin (mabcam8226; Abcam) for 60 minutes at RT. After the membranes were washed three times in TBST, donkey biotinylated anti-mouse IgG (Jackson ImmunoResearch Laboratories) was added for 30 minutes at room temperature. Protein bands were visualized (Vectastain ABC Elite Kit; Vector Laboratories, Burlingame, CA) with DAB (Vector Laboratories) as the substrate. The plot profile of the bands was analyzed with the NIH image 1.63 software with band density of AM sheets in each group standardized at 1.0.

Statistical Analysis

Statistical comparisons of Western blot band intensity, CFE, epithelialization, and BrdU and Ki67 staining were performed with the nonpaired Student's t-test (Excel; Microsoft, Redmond, WA).

RESULTS

Generation of Carrier-Free Epithelial Cell Sheets

Rabbit corneal epithelial cells were cultured with 3T3 feeder cells for 1 to 2 weeks, followed by airlift cultures to produce stratified epithelium on plastic coated with fibrin polymer (Fig. 1A). Fibrin remained at the bottom of the cell sheet when cultured with aprotinin (Figs. 1B, 1D) and was dissolved after removal of aprotinin, presumably due to intrinsic proteolytic activity (Figs. 1C, 1E).

In Vitro Characteristics of Cultivated Sheets

We performed a comparative study of carrier-free corneal epithelial sheets with epithelial sheet cultivated on AM carriers. Stratified epithelium was engineered on both AM (Fig. 2A) and plastic coated with degradable fibrin polymer (Fig. 2B). The use of aprotinin did not affect cell growth or stratification on the AM carriers.

Immunohistochemistry using anti-K3 and K12 antibodies showed that carrier-free cultures produced uniform layers of cells expressing both differentiation markers (Figs. 2C–F). Sporadic cells in the basal layer were K3 negative, which is characteristic of immature limbal basal cells in vivo. Both AM and carrier-free sheets expressed K14 (Figs. 2G, 2H) and p63 (Figs. 2I, 2J). The epithelium on AM carriers appeared to express higher levels of K14 and p63, and less K3, K12, suggesting that the AM maintains epithelial cells in a less differentiated state. The difference in K3 expression was also demonstrated by Western blot analysis (Figs. 2K, 2L). Both AM and carrier-free sheets show an intact superficial tight junction, as shown by immunohistochemistry of occludin (Figs. 3G, 3H) and the exclusion of HRP (Figs. 3I, 3J). Basement membrane components such as collagen IV and laminin were more prominent in the AM sheet in vitro (Figs. 3C, 3E). These proteins were not as evident in the carrier-free sheets before transplantation (Figs. 3D, 3F). However, the adhesion molecule integrin β1 was expressed in both sheets (Figs. 3A, 3B).

Transmission electron microscopy revealed that the ultrastructure of the epithelium was similar between the AM and carrier-free sheets, consisting of five to six layers of stratified epithelial cells with typical columnar basal cells and superficial cells with microvilli (Figs. 4A, 4B). Both cells sheets showed tight junction formation in apical cells (Figs. 4C, 4D) and desmosome formation (Figs. 4E, 4F). Although a basement membrane structure was observed in AM sheets (Fig. 4G), the carrier-free sheets showed residual material attached to the

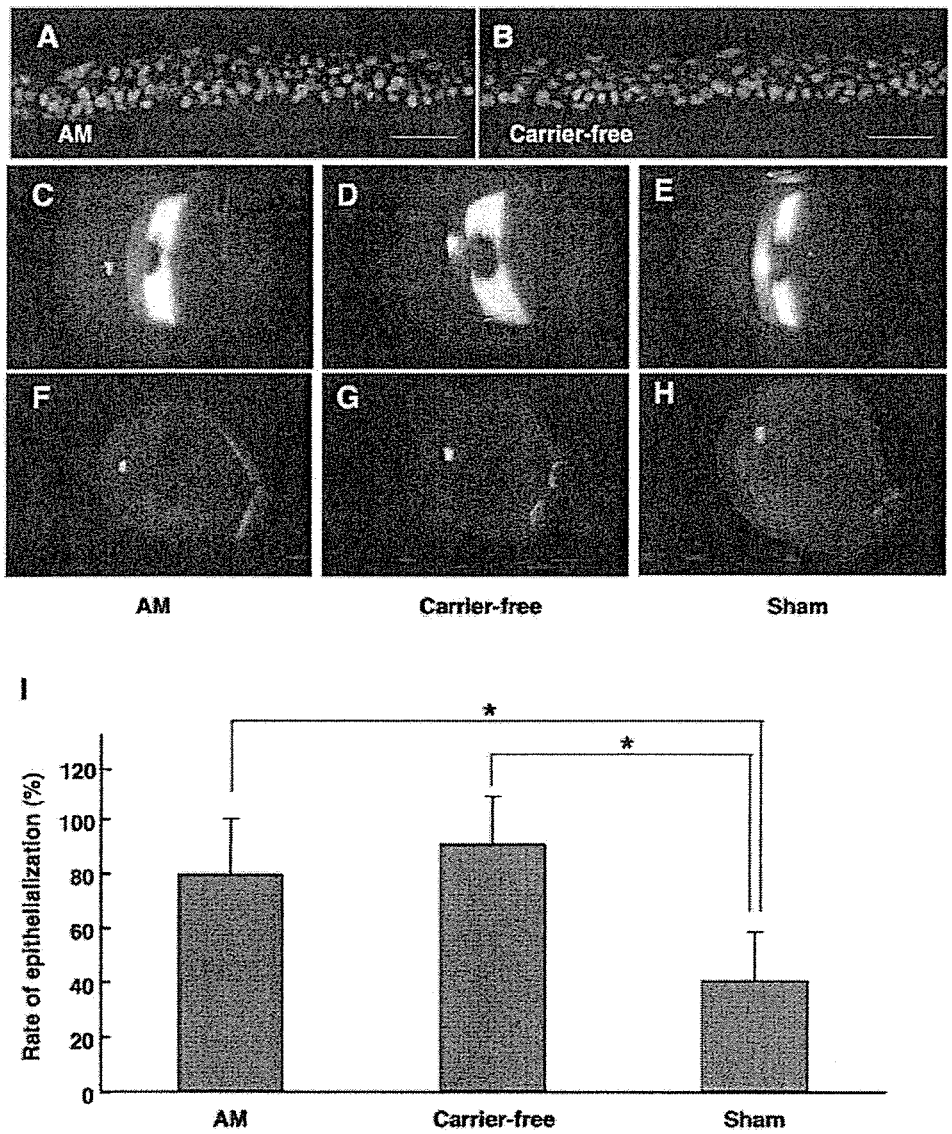

FIGURE 6. Epithelial sheet transplantation in rabbits. Immunohistochemistry of BrdU (A, B) in epithelial sheets before transplantation. Slit lamp photographs (C–E) and fluorescein staining (F–H) of rabbit eyes 1 week after epithelial sheet transplantation. (C, F) AM, (D, G) carrier-free, (E, H) sham. (I) Area of intact epithelium was larger in rabbit eyes after epithelial sheet transplantation compared with sham ($^*P < 0.05$). Carrier-free sheets had a smoother epithelial surface with minimal inflammation. Scale bar, 50 μm.

basal epithelial membrane (Fig. 4H) which may represent components of the basement membrane structure such as integrin β1, collagen IV, and laminin observed by immunohistochemistry (Figs. 3B, 3D, 3F).

Colony-Forming Efficiency

Isolated epithelial cells from both carrier-free (6.6% ± 1.2%) and AM carrier sheets (8.6% ± 2.7%) maintained the ability to form colonies in a 3T3 feeder layer (Figs. 5A, 5B). Although the number of large colonies (100 mm^2) was higher in AM sheets (AM: 2.8 ± 1.3 colonies, fibrin: 0.6 ± 0.8 colonies, $P = 0.014$, $n = 5$), the difference in the total number of colonies was not statistically significant (Fig. 5C).

Cultivated Sheet Transplantation

BrdU labeling was performed on the AM (Fig. 6A) and carrier-free (Fig. 6B) sheets before surgery, showing that most of the cells in both groups are viable with proliferative potential. Rabbits without cell sheet transplants characteristically had epithelial defects at 1 week after surgery, as shown by the positive staining with fluorescein dye in Figure 6H (dotted line). An intact epithelial layer excluded the dye in the AM (Fig. 6F) and carrier-free (Fig. 6G) sheet transplants. The irregular staining in the AM sheet corresponds to folds in the transplant. Optical clarity was higher in the carrier-free group (Fig. 6D) than in the group with AM sheet transplants (Fig. 6C). Rabbits in the AM sheet group also had inflammation of the conjunctiva due to the presence of sutures. The area of intact epithelium at 1 week after surgery was significantly higher in both AM (79.4% ± 20.4%) and carrier-free (90.7% ± 17.4%) epithelial sheet groups compared with the sham-surgery control (40.2% ± 18.3%, $P < 0.05$; Fig. 6I).

Immunohistochemistry of postoperative corneas showed normal K3 expression in the transplant sheets (Figs. 7C, 7D). Sham-surgery eyes exhibited partial epithelialization by K3-negative epithelium of conjunctival origin. Basement membrane components such as collagen IV were more prominent in the AM sheet group (Figs. 7E, 7F). Proliferation of transplanted cells was observed by the distribution of BrdU staining, which was uniformly present in cells before surgery. BrdU-positive cells were observed in both groups, indicating that these cells were of donor origin and were slow cycling during the 1-week period after surgery (Figs. 7G, 7H). The number of BrdU-positive cells in the AM group was significantly higher

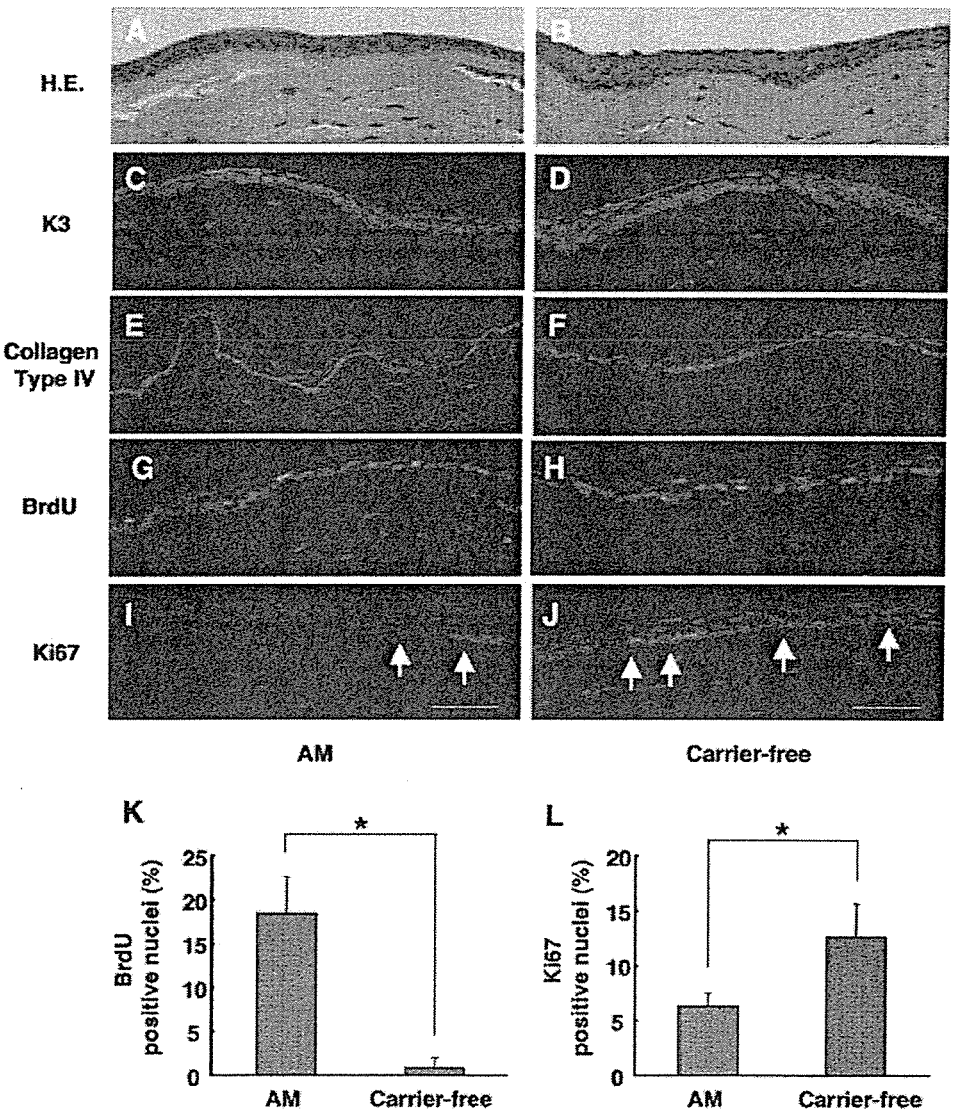

FIGURE 7. Postoperative histology of epithelial sheet transplantation. Light micrograph of hematoxylin and eosin–stained sections of AM (A) and carrier-free (B) epithelial sheets. Immunohistochemistry of K3 (C, D), Collagen type IV (E, F), BrdU (G, H), and Ki67 (I, J). AM sheets retained significantly higher levels of BrdU (K) and expressed lower levels of Ki67 (L) than did carrier-free sheets ($^*P < 0.05$, Student's *t*-test). Scale bar, 50 μm.

than that in the fibrin group (AM: 18.4% ± 4.2%, fibrin: 1.1% ± 1.1%, $P = 0.0002$, $n = 4$; Fig. 7K). Staining of the proliferation marker Ki67 was also observed in the basal layers of both groups (Figs. 7I, 7J), with significantly less Ki67-positive cells in the AM group than in the fibrin group (AM: 6.3% ± 1.2%, fibrin: 12.6% ± 3.1%, $P = 0.0087$, $n = 4$; Fig. 7L). BrdU- and Ki67-positive cells were uniformly distributed throughout the epithelial sheet in both groups, and there was no tendency of higher localization of label retaining cells in the limbus under the conditions of the study.

DISCUSSION

The homeostasis of cells undergoing constant turnover depends on the healthy supply of regenerating cells, as well as an intact interaction between surrounding tissues. In the case of the corneal epithelium, stem cells in the basal limbus supply transient amplifying (TA) cells to the corneal basal layer, which proliferate and slough off the ocular surface after approximately 2 weeks. The proliferation and differentiation of epithelial cells is regulated by stromal–epithelial interaction with keratocytes, the major mesenchymal cell in the corneal stroma. Chemokines and growth factors secreted by keratocytes are involved in the proliferation and differentiation of the overlying epithelium.[17] We found that although both AM sheets and carrier-free sheets were viable in transplant-recipient eyes, carrier-free transplants demonstrated a more robust layer of fully differentiated cells.

We observed more BrdU labeled cells and fewer Ki67-labeled cells in AM sheets compared with carrier-free sheets after transplantation. Previous studies have shown that cell-cycle kinetics and cell phenotype characteristic of limbal epithelial progenitor cells are preserved during ex vivo expansion on AM.[18,19] The difference in cell-cycle kinetics may be due to the presence of the AM basement membrane, which may modulate epithelial cell adhesion, proliferation, and differentiation.[18,20,21] In contrast, epithelial cells in carrier-free sheets seem to become integrated into the host tissue earlier, suggesting that the AM may be interfering with interactions between the epithelium and stromal cells. The absence of a carrier will restore epithelium–stromal interactions immediately after surgery, may have several advantages in maintaining a healthy epithelium, and may also allow the regeneration of a normal subepithelial nerve plexus. It can be argued that a larger yield of undifferentiated cells may be preferable in the treatment of stem cell–depleted cases. However, a mature corneal epithe-

lium is also required for the ocular surface to act as a barrier against invading organisms, as well as to provide a smooth surface for visual clarity. The clinical data available to date show that both AM sheets and carrier-free sheets can restore the epithelium for more than 1 year,[7,9] which would not be possible without the restoration of progenitor cells.

Another major benefit of carrier-free cell sheets is the surgical technique, which does not require the use of sutures for donor fixation. The mechanisms involved may be multiple, however, Nishida et al.[8] show that intact basement membrane substrates and adhesion molecules may play a major role. We have confirmed the presence of β1 integrin in the carrier-free group, which may have aided the carrier-free sheets in remaining on the ocular surface without sloughing off. In contrast, AM sheets require sutures for transplantation, and ingrowth of cells was observed under the AM carrier in several cases. These results show that attachment of cell sheets to the underlying stroma is stronger with carrier-free sheets during the early postoperative stage. Furthermore, the method we describe for engineering carrier-free sheets is different from previous approaches involving temperature-responsive dishes and does not require any specialized equipment or high levels of technical expertise.

The design of our study made use of rabbits with denuded epithelium, including the limbal area. We did not take into account any damage to the underlying stromal tissue, which is sometimes observed in clinical cases after severe chemical and thermal burns. The conclusions drawn from our study therefore should be interpreted as being based on epithelial sheet transplantation in situations with relatively intact stromal tissue. The AM is rich in basement membrane components since the amnion itself supports epithelial cells in the uterus. The use of an AM carrier may therefore have benefits in cases with extensive damage and inflammation in the underlying stroma.

There are still several issues to be resolved before the generalization of epithelial sheet surgery. The manufacture of stratified epithelial sheets requires the use of 3T3 feeder cells and culture-grade serum. Although adverse effects have not been reported, xeno-free techniques should be pursued. Similarly, the choice of whether to use carriers or not requires elucidation. Our data clearly show that cell sheets engineered without carriers reconstruct host tissue nearly to its original state as early as 1 week after surgery. Further refinements in surgical technique and quality control of cultured sheets should expand the therapeutic indications for tissue-engineered cell sheet transplantation.

Acknowledgments

The authors thank Mifuyu Oshima and Tomomi Sekiguchi for technical assistance and the staff of the Cornea Center Eye Bank for administrative support.

References

1. Kenyon KR, Tseng SC. Limbal autograft transplantation for ocular surface disorders. *Ophthalmology.* 1989;96:709–722; discussion 722–723.
2. Tsubota K, Satake Y, Kaido M, et al. Treatment of severe ocular-surface disorders with corneal epithelial stem-cell transplantation. *N Engl J Med.* 1999;340:1697–1703.
3. Pellegrini G, Traverso CE, Franzi AT, et al. Long-term restoration of damaged corneal surfaces with autologous cultivated corneal epithelium. *Lancet.* 1997;349:990–993.
4. Rama P, Bonini S, Lambiase A, et al. Autologous fibrin-cultured limbal stem cells permanently restore the corneal surface of patients with total limbal stem cell deficiency. *Transplantation.* 2001;72:1478–1485.
5. Koizumi N, Inatomi T, Quantock AJ, et al. Amniotic membrane as a substrate for cultivating limbal corneal epithelial cells for autologous transplantation in rabbits. *Cornea.* 2000;19:65–71.
6. Tsai RJ, Li LM, Chen JK. Reconstruction of damaged corneas by transplantation of autologous limbal epithelial cells. *N Engl J Med.* 2000;343:86–93.
7. Shimazaki J, Aiba M, Goto E, et al. Transplantation of human limbal epithelium cultivated on amniotic membrane for the treatment of severe ocular surface disorders. *Ophthalmology.* 2002;109:1285–1290.
8. Nishida K, Yamato M, Hayashida Y, et al. Functional bioengineered corneal epithelial sheet grafts from corneal stem cells expanded ex vivo on a temperature-responsive cell culture surface. *Transplantation.* 2004;77:379–385.
9. Nishida K, Yamato M, Hayashida Y, et al. Corneal reconstruction with tissue-engineered cell sheets composed of autologous oral mucosal epithelium. *N Engl J Med.* 2004;351:1187–1196.
10. Nakamura T, Endo K, Cooper LJ, et al. The successful culture and autologous transplantation of rabbit oral mucosal epithelial cells on amniotic membrane. *Invest Ophthalmol Vis Sci.* 2003;44:106–116.
11. Nakamura T, Inatomi T, Sotozono C, et al. Transplantation of cultivated autologous oral mucosal epithelial cells in patients with severe ocular surface disorders. *Br J Ophthalmol.* 04;88:1280–1284.
12. Itabashi Y, Miyoshi S, Kawaguchi H, et al. A new method for manufacturing cardiac cell sheets using fibrin-coated dishes and its electrophysiological studies by optical mapping. *Artif Organs.* 2005;29:95–103.
13. Espana EM, Romano AC, Kawakita T, et al. Novel enzymatic isolation of an entire viable human limbal epithelial sheet. *Invest Ophthalmol Vis Sci.* 2003;44:4275–4281.
14. Kim HS, Jun Song X, de Paiva CS, et al. Phenotypic characterization of human corneal epithelial cells expanded ex vivo from limbal explant and single cell cultures. *Exp Eye Res.* 2004;79:41–49.
15. Li DQ, Chen Z, Song XJ, et al. Partial enrichment of a population of human limbal epithelial cells with putative stem cell properties based on collagen type IV adhesiveness. *Exp Eye Res.* 2005;80:581–590.
16. Tseng SC, Kruse FE, Merritt J, Li DQ. Comparison between serum-free and fibroblast-cocultured single-cell clonal culture systems: evidence showing that epithelial anti-apoptotic activity is present in 3T3 fibroblast-conditioned media. *Curr Eye Res.* 1996;15:973–984.
17. Wilson SE, Mohan RR, Mohan RR, et al. The corneal wound healing response: cytokine-mediated interaction of the epithelium, stroma, and inflammatory cells. *Prog Retin Eye Res.* 2001;20:625–637.
18. Grueterich M, Espana E, Tseng SC. Connexin 43 expression and proliferation of human limbal epithelium on intact and denuded amniotic membrane. *Invest Ophthalmol Vis Sci.* 2002;43:63–71.
19. Meller D, Pires RT, Tseng SC. Ex vivo preservation and expansion of human limbal epithelial stem cells on amniotic membrane cultures. *Br J Ophthalmol.* 2002;86:463–471.
20. Jones PH, Harper S, Watt FM. Stem cell patterning and fate in human epidermis. *Cell.* 1995;80:83–93.
21. Li W, He H, Kuo CL, et al. Basement membrane dissolution and reassembly by limbal corneal epithelial cells expanded on amniotic membrane. *Invest Ophthalmol Vis Sci.* 2006;47:2381–2389.

Dendritic Keratitis Caused by an Acyclovir-Resistant Herpes Simplex Virus With Frameshift Mutation

Wei Zhang, MD, PhD, Takashi Suzuki, MD, PhD,* Atsushi Shiraishi, MD, PhD,* Ichiroh Shimamura, MD,* Yoshitsugu Inoue, MD, PhD,† and Yuichi Ohashi, MD, PhD**

Purpose: To report a case of acyclovir-resistant herpes simplex virus (HSV) keratitis after long-term, inconsistent use of topical acyclovir and fluorometholone.

Methods: A 70-year-old man with dendritic keratitis caused by an acyclovir-resistant HSV strain was examined. The 50% inhibitory concentration of different antiviral agents against the isolated virus and the DNA sequence of viral thymidine kinase were determined.

Results: The 50% inhibitory concentration of acyclovir and trifluorothymidine for the isolated HSV strain was 13.75 and 0.28 μg/mL, respectively, indicating that the virus was resistant to acyclovir. DNA sequencing of the viral thymidine kinase revealed that this virus had a frameshift mutant with a G insertion in the 7Gs homopolymer. Topical trifluorothymidine was effective, and the epithelial lesion was completely resolved within 2 weeks.

Conclusion: A typical form of dendritic keratitis was caused by an acyclovir-resistant HSV with frameshift mutation in a 7Gs homopolymer region.

Key Words: acyclovir resistance, keratitis, frameshift mutation, herpes simplex virus, thymidine kinase

(*Cornea* 2007;26:105–106)

Herpes simplex keratitis is still 1 of the leading causes of infectious corneal blindness in the world. Acyclovir (ACV) ointment has been extensively used as the first choice drug of herpes simplex keratitis in Japan because of its high antiviral efficacy and low cytotoxicity. This treatment has resulted in a significant reduction of patients who develop necrotizing stromal keratitis and corneal perforations.

However, the widespread use of ACV has invariably led to the emergence of herpes simplex virus (HSV) strains resistant to ACV, especially in severely immunocompromised patients. During the past several years, ACV-resistant HSV strains have been isolated from various sites including the eye. Three mechanisms may be involved in the development of ACV-resistant HSV: a loss of thymidine kinase (TK) activity (TK-deficient virus), an alteration of TK activity or substrate specificity (TK-altered virus), and an alteration of DNA polymerase activity. In 95% of the cases, ACV resistance is associated with a mutation in the *TK* gene.[1]

We report a case of dendritic keratitis that did not respond to topical ACV ointment. A novel frameshift mutation was detected in this ACV-resistant, ocular HSV isolate.

CASE REPORT

A 70-year-old, immunocompetent man was referred from a local hospital in March 2005 for recurrent dendritic keratitis that had been treated unsuccessfully with topical ACV. He complained of redness, irritation, pain, and blurred vision in his right eye. His best-corrected visual acuity was reduced to 20/25 in the affected eye. Slit-lamp examination showed dendritic keratitis with slight stromal edema but no significant signs of anterior chamber inflammation.

The epithelial lesion was found to develop at the lower portion of the cornea, a part of which was geographic in appearance (Fig. 1). Suspecting poor compliance, we gave the patient strict instructions on the use of ACV ointment 5 times a day for 1 week, but no improvement was observed. The patient had a 10-year history of recurrent dendritic and disciform keratitis and had been given topical ACV with fluorometholone for a long time, but his compliance was poor.

We considered the possibility of an ACV-resistant HSV; corneal epithelial debridement was performed under local anesthesia for virus isolation. Typical cytopathic effect was observed on the next day, and the isolated virus was identified as HSV-1 by indirect immunofluorescence. As reported previously,[2] antiviral plaque reduction assay was performed with ACV, trifluorothymidine (TFT), foscarnet (FOS), and idoxuridine (IDU) to determine the 50% viral inhibitory concentration (IC_{50}). As a result, the IC_{50} of this strain against ACV, TFT, and FOS was 13.75, 0.28, and 7.14 μg/mL, respectively. No plaque reduction occurred at any concentration of IDU. Generally, in an antiviral plaque reduction assay, HSV with IC_{50} exceeding 2 μg/mL to ACV is considered resistant.[3] The IC_{50} of this strain was 13.75 μg/mL, indicating that the dendritic keratitis was caused by an ACV-resistant HSV strain.

We therefore discontinued topical ACV and switched to 1% topical TFT, which this strain was sensitive to. The patient was given 1% topical TFT 8 times per day, and the 1% TFT solution was prepared in our facility from TFT (Sigma, St. Louis, MO). The epithelial lesion healed completely within 2 weeks.

The analysis of the *TK* gene of the isolated virus strain was performed as described[4] and compared with the *TK* gene of an ACV-sensitive clinical isolated from a patient with dendritic keratitis. A G insertion in a homopolymer harboring 7 Gs was detected in the TK

Received for publication April 17, 2006; accepted for publication July 2, 2006.

From the *Department of Ophthalmology, Ehime University School of Medicine, Shitsukawa, Toon-City, Ehime, Japan; and the †Division of Ophthalmology and Visual Science, Faculty of Medicine, Tottori University, Yonago, Japan.

Reprints: Wei Zhang, Department of Ophthalmology, Ehime University School of Medicine, Shitsukawa, Toon-City, Ehime 791-0295, Japan (e-mail: zhangwei@m.ehime-u.ac.jp).

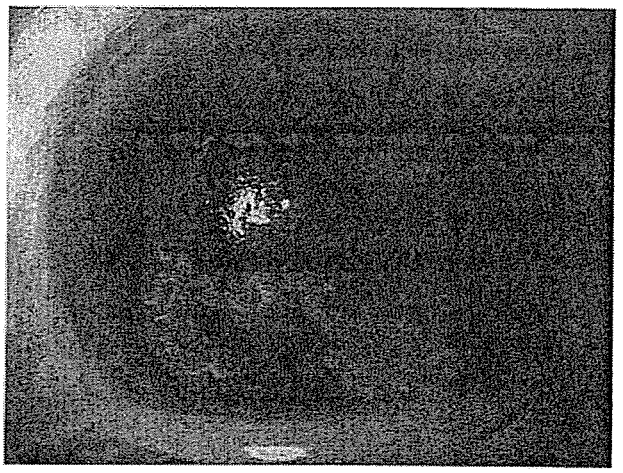

FIGURE 1. Slit-lamp photograph of right eye with fluorescein staining showing typical dendritic keratitis with a part of geographic in appearance at the lower portion of the cornea.

sequence. This insertion was located at nucleotides 429 to 436 (codon 144–146), causing a premature stop codon at 227 (Table 1).

TABLE 1. TK Gene Sequence

	Nucleotide Change	Amino Acid Change
Isolated virus	125: C→T	42: Pro→Leu
	256: G→A	89: Arg→Gln
	437: ins G	146: frameshift
		227: stop codon

DISCUSSION

Among the mutations that are associated with ACV resistance, one half are nucleotide insertions or deletions and the other half are nucleotide substitutions. Generally, such mutants have low virulence. For example, Yao et al[2] have reported 2 ACV-resistant HSV-1 mutants with a nucleotide substitution, and both had low virulence in the cornea and had a low incidence of establishing a latent infection. One had a point mutation in the ATP binding site (codon 55) of the *TK* gene, whereas the other was in codon 125.

Nucleotide insertions or deletions are usually responsible for a frameshift resulting in the synthesis of a truncated, nonfunctional TK. A mutant strain with a frameshift mutation within the 7 Gs homopolymers, however, could synthesize a part of a full-length TK because of an unusual net +1 frameshift during translation. This outcome first reported in a patient with progressive esophagitis that had developed after bone marrow transplantation. It was noted that the mutant retained some TK activity and had the ability to reactivate from latent infections in the mouse trigeminal ganglia.[5] In fact, recurrences have occurred in a bone marrow transplant patient.[6] Thus, net +1 frameshift mutants have stronger virulence and higher rate of recurrences than the more common mutants because of their specific process of translation. Our mutant also possessed strong virulence, causing typical dendritic keratitis and the ability to establish latency[5] (Zhang et al, unpublished data).

ACV-resistant mutants of HSV emerge predominantly in severely immunocompromised patients (eg, bone marrow transplants, cancer, and AIDS).[1] Although resistance to ACV rarely occurs among immunocompetent patients, there have been several reports of ACV-resistant herpes simplex keratitis in otherwise healthy individuals.[4] This finding is probably attributable to the inherent immunocompromised status of the cornea because of its avascularity. Our patient was immunocompetent according to his medical history. Therefore, we presume that the long-term, irregular concomitant use of a low dose of ACV and steroids is responsible for the emergence of this ACV-resistant mutant. Although sensory ganglia harboring latent HSV-1 are not generally reinfected with a second strain of HSV-1, superinfection has been reported to occur.[7,8] Because the strain we reported here can establish latency[5] (Zhang et al, unpublished data), a possibility of recurrence, albeit remote, should be kept in mind.

REFERENCES

1. Morfin F, Thouvenot D. Herpes simplex virus resistance to antiviral drugs. *J Clin Virol*. 2003;26:29–37.
2. Yao YF, Inoue Y, Kase T, et al. Clinical characteristics of acyclovir-resistant herpetic keratitis and experimental studies of isolates. *Graefes Arch Clin Exp Ophthalmol*. 1996;234:126–132.
3. Englund J, Zimmerman ME, Swierkosz EM, et al. Herpes simplex virus resistant to acyclovir: a study in a tertiary care center. *Ann Intern Med*. 1990;112:416–422.
4. Bodaghi B, Mougin C, Michelson S, et al. Acyclovir-resistant bilateral keratitis associated with mutations in the HSV-1 thymidine kinase gene. *Exp Eye Res*. 2000;71:353–359.
5. Hwang CB, Horsburgh B, Pelosi E, et al. A net +1 frameshift permits synthesis of thymidine kinase from a drug-resistant herpes simplex virus mutant. *Proc Natl Acad Sci USA*. 1994;91:5461–5465.
6. Morfin F, Thouvenot D, Aymard M, et al. Reactivation of acyclovir-resistant thymidine kinase-deficient herpes simplex virus harbouring single base insertion within a 7 Gs homopolymer repeat of the thymidine kinase gene. *J Med Virol*. 2000;62:247–250.
7. Landry ML, Zibello TA. Ability of herpes simplex virus (HSV) types 1 and 2 to induce clinical disease and establish latency following previous genital infection with the heterologous HSV type. *J Infect Dis*. 1988;158:1220–1226.
8. Remeijer L, Maertzdor J, Buitenwerf J, et al. Corneal herpes simplex virus type 1 superinfection in patients with recrudescent herpetic keratitis. *Invest Ophthalmol Vis Sci*. 2002;43:358–363.

Marx Line: Fluorescein Staining Line on the Inner Lid as Indicator of Meibomian Gland Function

MASAHIKO YAMAGUCHI, MD, MIKI KUTSUNA, MD, PHD, TOSHIHIKO UNO, MD, PHD, XIAODONG ZHENG, MD, PHD, TOSHIO KODAMA, MD, PHD, AND YUICHI OHASHI, MD, PHD

• PURPOSE: To determine whether the location of a fluorescein-stained line, the Marx line (ML), which runs along the inner eyelid, is correlated with meibomian gland function.

• DESIGN: Prospective observational case series.

• METHODS: After applying fluorescein dye solution to the eye, the ML score was calculated for the outer, middle, and inner thirds of the lower eyelid margin. ML scoring was as follows: 0, entirely on the conjunctival side of the meibomian orifices (MOs); 1, part of the ML touches the MOs; 2, ML runs through all of the MOs; and 3, ML runs on the eyelid-margin side of the MOs. Correlations were calculated between the total ML score and age for 251 randomly recruited subjects without acute ocular surface diseases, and between age and the ML score for the three regions of the lower eyelid. Correlations between the regional ML score and the meibographic score, and the meibomian gland secretion score were also determined. The total ML scores of 15 subjects without meibomian gland dysfunction (MGD) were compared with 15 age-matched patients with MGD.

• RESULTS: The three regions of the lower eyelid had significantly different ML scores. Strong correlations were found between the ML score and age, the meibographic score, and the meibomian gland secretion score. The total ML score of MGD group was significantly higher than that of the non-MGD group.

• CONCLUSIONS: The strong correlation between the ML score and the meibomian gland scores indicates that the ML score can be used as a simple and rapid screening score for meibomian gland function. (Am J Ophthalmol 2006;141:669–675. © 2006 by Elsevier Inc. All rights reserved.)

Accepted for publication Nov 8, 2005.

From the Department of Ophthalmology, University of Ehime School of Medicine, Ehime, Japan.

Inquiries to Masahiko Yamaguchi, MD, Shitsukawa, Toon City, Ehime, 791-0295 Japan; e-mail: masahiko@m.ehime-u.ac.jp

LIPIDS SECRETED FROM THE MEIBOMIAN GLANDS spread over the ocular surface by blinking and form the outer layer of the tear film to suppress evaporation.[1] These lipids also form a hydrophobic barrier at the eyelid margin that prevents the loss of tear fluid.[2] Because these two mechanisms are important for maintaining the stability of tear film, evaluation of meibomian gland function is essential when investigating the cause or treating dry eye patients.

There is a wide range of clinical examination, from simple and fast to comprehensive and time-consuming, designated to evaluate meibomian gland function. These include routine slit-lamp observations of the meibomian orifices (MOs), examination of meibomian gland sebum,[3] meibography that assesses the structure of the glands by transillumination,[4–6] meibometry that measures lipid secretion of the glands,[7,8] and analysis of meibomian gland lipids by thin-layer chromatography.[9,10] Although these methods are all valuable, a simpler test that could rapidly and accurately screen meibomian gland function is still needed for routine clinical practice.

When a fluorescent dye solution is applied to the eyelid margin, a clear line, called the Marx line (ML),[11] is recognizable, running along the inner eyelid. In normal eyes, this line is located on the conjunctival side of the MOs; however, depending on the case, the ML may be totally or partially located on the cutaneous side of the MOs.

We have hypothesized that changes in the location of the ML might be correlated with meibomian gland function. To test this hypothesis, we have determined the correlations between the ML scores and the results of more conventional tests of meibomian gland function. We also investigated the effects of aging and regional changes in the ML scores in subjects with meibomian gland dysfunction (MGD).

METHODS

THE PURPOSE OF THIS STUDY AND THE PROCEDURES TO BE used were presented to all of the subjects and patients, and

0002-9394/06/$32.00
doi:10.1016/j.ajo.2005.11.004

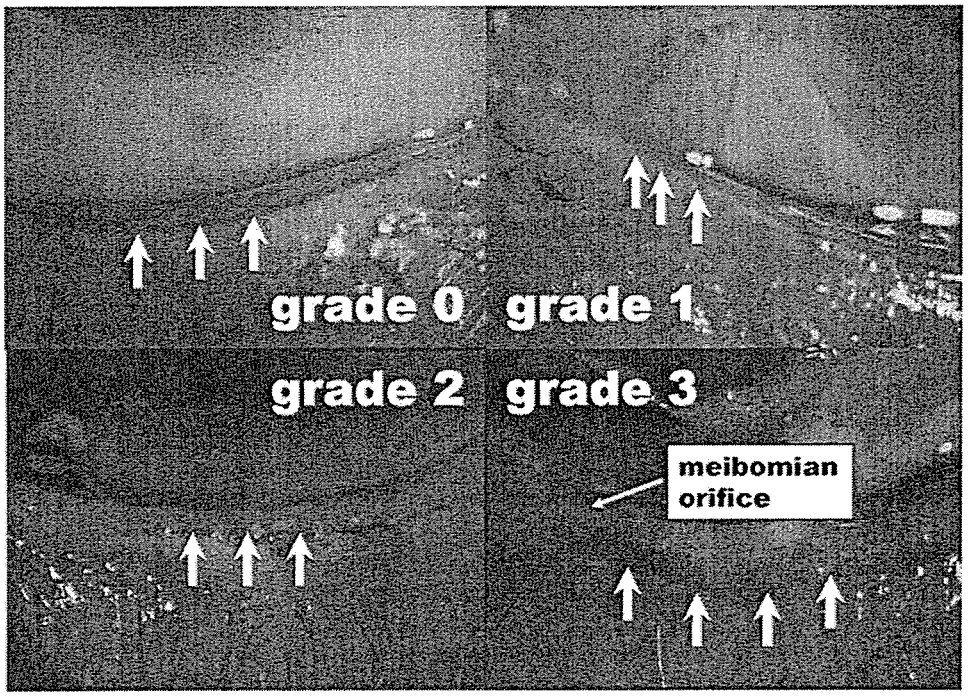

FIGURE 1. Marx line (ML) (arrows) scores: 0, fluorescein staining line running entirely along the conjunctival side of the meibomian orifices (MOs); 1, parts of the ML touching the MOs; 2, ML running through the MOs; and 3, ML running along the eyelid margin side of the MOs.

signed informed consent was obtained from each individual. The procedures used in this study conformed to the tenets of the Declaration of Helsinki.

A total of 251 subjects (105 men and 146 women, ages 59.8 ± 20.3 years [mean ± SD]) were randomly recruited from the patients who were treated at the Department of Ophthalmology of Ehime University Hospital, Ehime, Japan. None of these subjects had acute ocular surface disorders, trauma, infections, or immune diseases, such as Stevens-Johnson syndrome or ocular cicatricial pemphigoid.

The correlation between the total ML score (see below) and age was determined for the 251 subjects. In addition, among the 251 subjects, a panel of randomly selected 65 subjects (30 men and 35 women, ages 52.0 ± 23.3 years) was analyzed to determine whether a significant correlation existed between the ML score in the upper and lower eyelids. A panel of randomly selected 116 subjects (51 men and 65 women, ages 56.7 ± 17.0 years) was studied to compare the ML scores to the scores of the meibography, and another panel of 126 subjects (60 men and 66 women, ages 44.3 ± 20.2 years) was studied to compare the ML scores to the scores of the meibomian gland secretion.

To demonstrate the ML, 2 μl of fluorescein 1% solution, lissamine green B 1% solution, or rose bengal 1% solution was instilled separately into the lower fornix in 10 subjects, and after the patient blinked a few times, a stained line was observed by slit-lamp biomicroscopy along the lower eyelid. The fluorescein 1% solution was prepared by diluting fluorescein 10% solution (Fluorescite; Alcon Lab Inc, Fort Worth, Texas, USA) in saline; the lissamine green B 1% solution was prepared by dissolving lissamine green B bulk powder (Sigma Chemical Co, St Louis, Missouri, USA) in saline; and the rose bengal 1% solution was prepared by dissolving rose bengal bulk powder (Wako) in a mixture of ethyl paraoxybenzoine and propyl paraoxybenzoine. All of the solutions were sterilized by filtration through a 0.22-μm Millipore filter. There were no clinically significant adverse reactions caused by any of the solutions.

After fluorescein staining, the lower lid was examined by slit-lamp biomicroscopy, and a score was assigned according to the following criteria: 0, ML runs entirely along the conjunctival side of the MOs: 1, parts of the ML touch the MOs; 2, the ML runs through the MOs; and 3, the ML runs along the eyelid-margin side of the MOs (Figure 1).

The lower eyelid was further divided into three portions; the outer third, middle third, and inner third (Figure 2). The sum of the ML scores for the three portions of the lower lid was defined as the total score of each eye; the maximum possible ML score was 9. The mean total score was obtained by averaging ML scores of the lower eyelids of both eyes.

To estimate the accuracy of this scoring system, 20 representative photographs of the ML were individually presented to five ophthalmologists at our institution in a masked fashion, and the ML for the middle third of the lower lid was scored. As expected, the ML score for the 20 images was found to be reasonably consistent among the five ophthalmologists.

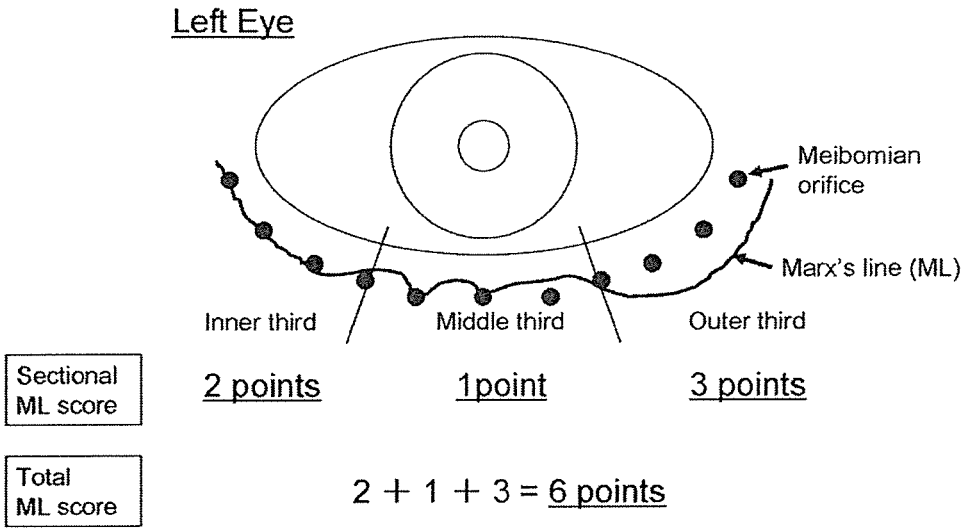

FIGURE 2. Calculation of the total ML score based on the regional scores: if the scores of the inner, middle, and outer thirds of the left eye are 1, 2, and 3, respectively, the total ML score is the sum of 1, 2, and 3, or 6 in this example.

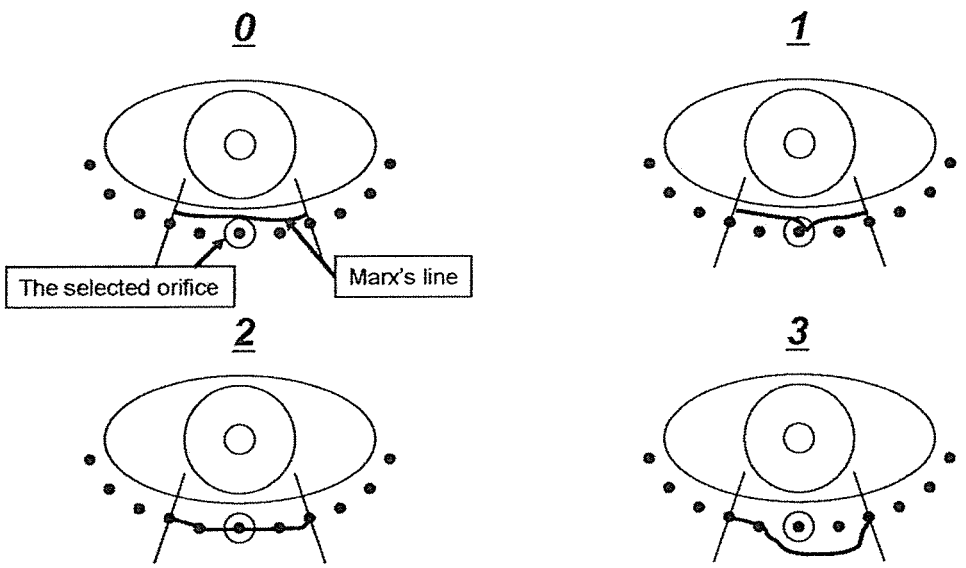

FIGURE 3. One MO was randomly selected in the center of the middle third of the lower eyelid and was scored by the ML scoring method.

Meibography, a morphologic examination of the meibomian glands that uses transillumination by a vitrectomy light probe,[4-6] was performed on one randomly selected eye of a panel of 116 subjects (51 men and 65 women, ages 56.7 ± 17.0 years). Clinical score was obtained at the outer, middle, and inner thirds of the lower eyelid according to the grading reported previously[5]: 0, no glandular loss; 1, glandular loss in less than half of each section; and 2, glandular loss in more than half of each section. Although the observation at the middle section of the lower eyelid is generally enough for screening, each of the three sections of the lower eyelid was examined as mentioned above for a more comprehensive evaluation. Then a correlation between the regional ML scores and the regional meibography scores was evaluated.

The secretion of the meibomian glands was examined in one randomly selected eye of a panel of 126 subjects (60 men and 66 women, ages 44.3 ± 20.2 years [mean ± SD]). One MO at approximately the center of the middle third of the lower eyelid was selected and its middle third ML scored, because digital pressure could be firmly and easily applied here (Figure 3). After compressing the selected meibomian gland, the color and viscosity of the secretions were scored as follows: 0, clear secretions with normal viscosity; 1, slightly yellowish with normal viscosity; 2, yellowish-white and opaque secretion with increased vis-

FIGURE 4. The lower eyelid margin was stained with fluorescein, lissamine green B, and rose bengal. The mucocutaneous junction is clearly stained by each solution at the same site. MO = meibomian orifice; MI = meibomian infarction.

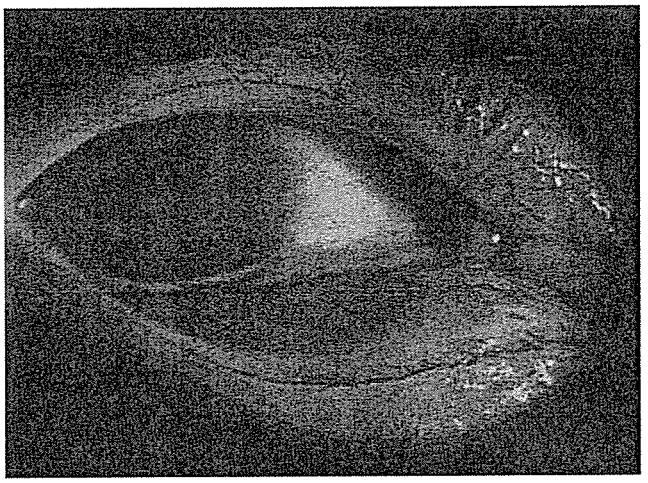

FIGURE 5. The MLs of the upper and lower eyelids are almost identical in most subjects.

cosity; 3, white and thick with a consistency of toothpaste; and 4, no secretions on compression. Then a correlation between the middle ML score and the score for the meibomian gland secretions was evaluated.

Apart from the original group of 251 subjects, the ML scores of 15 subjects (seven men and eight women, ages 44.2 ± 21.0 years) with MGD were compared with those from 15 age-matched subjects (seven men and eight women, ages 44.1 ± 20.0 years) without MGD. The subjects without MGD were defined as patients without acute ocular surface disease who had scores of one or less for the meibomian gland secretions. In the MGD group, the MOs were plugged and the meibomian gland secretion scores were two or more in all of the subjects. No one in the MGD group had been diagnosed with acute ocular surface disease.

The correlations between regional ML scores and meibography scores and between ML scores and meibomian gland secretions scores were analyzed by the Kruskal-Wallis test for analysis of variance and nonparametric Spearman rank correlation analysis among multiple groups. The

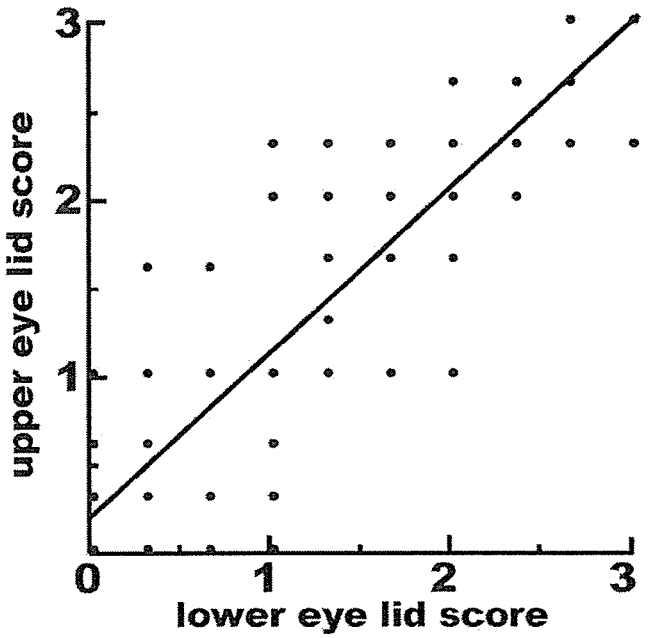

FIGURE 6. The correlation between the mean score of three parts (inner, middle, and outer thirds) for the upper eyelid and that of the lower eyelid was plotted. X axial = mean score of lower eyelid; Y axial = mean score of upper eyelid.

significance of the differences in the regional (inner, middle, outer) ML scores in different age groups was examined by the Kruskal-Wallis test for analysis of variance and the Scheffé *F* test for comparisons. The significance of differences in the total ML scores of eyes with and without MGD was determined by the Student *t* test.

RESULTS

AMONG FIVE OPHTHALMOLOGISTS, INCONSISTENCY OF A score was settled in less than one for the ML score, and scores did not differ by two or more for all 20 images. There was 100% coincidence in 8 (40%) of 20 images, 80%

TABLE 1. Correlation Between Marx Line Score and Meibographic Score*

Meibographic Score	Marx Line Score			
	0	1	2	3
0	45	40	10	0
1	40	50	39	39
2	0	0	26	59

*A total of 348 regions in 116 subjects were studied. Regional Marx line was scored 0 to 3 (horizontal line), and regional meibography was scored 0 to 2 (vertical line).

TABLE 2. Correlation Between Marx Line Score and Meibomian Gland Secretion Score*

Meibomian Gland Secretion Score	Middle Marx Line Score			
	0	1	2	3
0	22	6	5	0
1	7	12	14	5
2	2	12	10	20
3	0	2	3	3
4	0	0	0	3

*A total of 126 meibomian orifices in 126 eyes were studied. Middle third Marx line was scored 0 to 3 (horizontal line), and meibomian gland secretions of one meibomian orifice at approximately the center of the middle third of the lower eyelid was scored 0 to 4 (vertical line) correspondingly.

coincidence in 10 (50%) of 20 images, and 60% coincidence in all 20 images.

The staining pattern of the eyelid margin with fluorescein is shown in Figure 4. A sharply defined line can be seen on the inner eyelid, and the staining with rose bengal and lissamine green B solutions was almost consistently seen along this particular line (Figure 4), indicating that this line appeared to represent the mucocutaneous junction (MCJ). Because fluorescein is used much more widely than rose bengal or lissamine green B solutions in clinical practice, we chose to use fluorescein alone for the staining of lid margin in subsequent assessments.

The fluorescein-stained line was observed on the inner surface of both the upper and lower eyelids with a similar pattern (Figure 5). When the ML scores of the upper and lower eyelids were determined in 65 subjects, the regression line relating the mean score of three parts (inner, middle, and outer thirds) for the upper eyelid to that of the lower eyelid was as follows: [mean score of upper eyelid = 0.234 + 0.914 × mean score of the lower eyelid] (R^2 = 0.794; $P < .0001$, Figure 6). Because of this significant correlation, we decided to evaluate the ML score of the lower eyelid alone in the subsequent study. In addition, a strong positive correlation was also found in the mean ML scores for the inner, middle, and outer thirds of the upper eyelid to those of the lower eyelid (data not shown).

To determine the correlation between ML score and other tests of meibomian gland function, we first compared ML score with the meibography score in 116 subjects. The mean ± SD meibography scores for individuals with ML scores of 0, 1, 2, and 3 were as follows: 0.47 ± 0.50, 0.55 ± 0.50, 1.21 ± 0.66, and 1.60 ± 0.49, respectively. A strong positive correlation was found between the regional ML scores and the regional meibography scores (Kruskal-Wallis test, $P < .0001$; nonparametric Spearman rank correlation analysis, $r = 0.643$, $P < .0001$; Table 1).

Next, the mean ± SD meibomian gland secretion scores for the 126 subjects with middle third ML scores of 0, 1, 2, and 3 were 0.35 ± 0.61, 1.31 ± 0.86, 1.34 ± 0.87, and 2.13 ± 0.81, respectively. A strong positive correlation was also found between ML scores and meibomian gland secretion scores (Kruskal-Wallis test: $P < .0001$; nonparametric Spearman rank correlation analysis: $r = .599$, $P < .0001$; Table 2).

Effect of aging on the ML scores was determined for the 502 eyes of 251 subjects without acute ocular surface diseases. Correlation between the total ML score and age, and the correlations between ML score for the three segments of the lower lid and age were determined.

A strong positive correlation was found between the total ML score and age in both men and women (men, $R^2 = .548$; $P < .0001$; women, $R^2 = .588$; $P < .0001$). A strong positive correlation was also found between age and the score for the outer third of the lower eyelid in both men and women (men, $R^2 = .549$; $P < .0001$; women, $R^2 = .622$; $P < .0001$); for the inner third (men, $R^2 = .446$; $P < .0001$; women, $R^2 = .425$; $P < .0001$); and for the middle third (men, $R^2 = .364$; $P < .0001$; women, $R^2 = .344$; $P < .0001$).

The mean ± SD ML scores for the outer, middle, and inner thirds of the lower eyelid were also determined for the following three groups: subjects younger than 40 years (group 1), subjects from 41 to 60 years (group 2), and subjects older than 61 years (group 3). For group 1, ML score was 0 for the three regions in men and 0.14 ± 0.35, 0.09 ± 0.29, and 0.09 ± 0.29 in women. For group 2, the respective values were 1.05 ± 1.25, 0.34 ± 0.56, and 0.39 ± 0.63 in men, and 0.86 ± 0.95, 0.33 ± 0.53, and 0.39 ± 0.47 in women. For group 3, the values were 2.42 ± 0.85, 1.18 ± 0.87, and 0.68 ± 0.89 in men and 2.55 ± 0.80, 1.18 ± 0.94, and 1.54 ± 1.09 in women. More specifically, the scores for the outer third of lower eyelid were higher in both men and women.

There were no significant differences of the regional ML scores between men and women regarding to age. No difference of the ML scores was observed between the three regions in both men and women from group 1, but differences were observed between the three regions for both men and women in groups 2 and 3 (Kruskal-Wallis tests, $P < .0001$ and $P < .0001$, respectively). In group 2,

TABLE 3. Significance of Marx Line Scores for the Outer, Middle, and Inner Lower Eyelid Regions in Men and Women in Three Age Groups*

Group	Group 1 (≦40 years)	Group 2 (41–60 years)	Group 3 (≧61 years)
Men			
Inner vs middle	NS	NS	<.005
Inner vs outer	NS	NS	<.0001
Middle vs outer	NS	<.05	<.0001
Women			
Inner vs middle	NS	NS	NS
Inner vs outer	NS	<.05	<.0001
Middle vs outer	NS	<.0001	<.0001

Inner = Marx line score for the inner lower eyelid region; Middle = Marx line score for the middle lower eyelid region; Outer = Marx line score for the outer lower eyelid region; ns = no significant difference.
*Scheffé *F* test.

a difference of the scores was observed between the middle and outer thirds among men, as well as between the inner and outer thirds and the outer and middle thirds among women. In group 3, a difference of the scores was observed between any two of the regions, except for the inner and middle thirds in women (Table 3).

The mean ± SD ML scores for eyes in the non-MGD group and the MGD group were 2.77 ± 1.59 and 5.93 ± 1.55, respectively. The difference between these two groups was statistically significant ($P < .001$).

DISCUSSION

THE CONCEPT OF AN EVAPORATIVE TYPE OF DRY EYE[12] HAS become widely recognized as a result of better understanding of the pathogenesis of MGD in recent years. The importance of assessing meibomian gland function has been emphasized because lipids secreted by these glands combine with outer layers of the tear film not only to suppress evaporation of tear fluid, but also to form a hydrophobic barrier at the lid margin to prevent loss of tears.[1,2] Focusing on the latter role, we assume that the ML as revealed by fluorescein staining along the lid margin may represent such a barrier line. Because ML appears to be the interface between lipids secreted from the meibomian glands and the aqueous tear fluid, it may well be an indicator of meibomian gland function. The significance of ML was first pointed out by Norn,[13] who performed vital staining of the eyelid margin with fluorescein, lissamine green B, and Sudan III, and concluded that the stained line representing the border between tear fluid and the skin corresponded to the MCJ. In this study, we have reconfirmed Norn's observation as stated above and decided to use fluorescein for defining ML.

We have shown that the change of the location of this line was strongly correlated with meibomian gland function. We base this on the following: eyes with abnormal meibomian gland secretions or morphology had significantly higher ML scores; and ML scores were significantly higher in the MGD group than those in the group without MGD for age-matched subjects. Although a variety of methods or clinical techniques are being used to assess meibomian gland function, most of these procedures are either subjective or require special equipment. Our results demonstrated that scoring of the location of ML could be used as a rapid, efficient, less-invasive screening test for and assess of meibomian gland function. One great advantage of this procedure is that the information on the location of ML can be easily obtained during the fluorescein staining procedure in routine slit-lamp examination for patients with dry eye. Although the scoring and assessment of ML itself could be somehow subjective, the variation of the clinical score among experienced ophthalmologists was found to be reasonable and within an acceptable range.

The ML was found to shift gradually toward the outside of the eyelid margin with aging. That is, the ML generally runs in parallel and some distance away from the MOs along the conjunctival border in younger subjects. However, it becomes irregular and creeps closer to the MOs with aging, and finally extends beyond them in some subjects. This finding was consistent with the results obtained by Norn,[13] who had reported that the MOs were situated in a straight row just in front of the ML in younger normal subjects. However, the orifices were more often displaced in elderly normal subjects (>50 years)—that is, the ML might run an irregular course with increasing age.

When the ML of the inner, middle, and outer thirds of the lower eyelid was scored separately, it was found that the outward shift of the ML started earlier from the inner or outer third than the middle third, and such a shift was more common at the outer third in the elder individuals. This finding may imply that MGD are prone to develop in the inner or outer regions earlier, which is consistent with our finding that the meibomian glands at these regions are shorter and less well-developed as compared with those in the central region (data not shown). The involvement of conjunctivochalasis on the extensive outward shift of ML in elder population cannot be completely ruled out as this abnormality also occurs with aging and the redundant bulbar conjunctiva preferentially hang over the inner or outer third of the lid margin. In fact, there exists the possibility that the ML location might be modified when the lid margin become wet as a result of excessive bulbar conjunctiva. Nevertheless, ML score could still be a useful indicator for meibomian gland function unless a high degree of conjunctivochalasis is present.

In contrast to our observation, Hykin and Bron[14] reported that there were no age-related changes in the position and form of the MCJ in subjects without ocular

surface disorders. In addition, Bron and associates[15] reported that there existed two patterns of the MCJ location in eyes with MGD: an anteroplacement and a retroplacement. Especially, a retroplacement refers to a shift of the MCJ to the conjunctival side and was considered more common in eyes with MGD. We speculate that such a change might occur in patients with atopic dermatitis or other ocular surface disorders. Further careful survey would disclose this discrepancy.

In conclusion, we have demonstrated that the ML, the fluorescein staining line along the lower lid margin, is a good indicator of meibomian gland function. The evaluation is effective, less invasive, and practical as an easy screening test in daily clinical practice.

REFERENCES

1. Mishima S, Maurice DM. The oily layer of the tear film and evaporation from the corneal surface. Exp Eye Res 1961;1: 39–45.
2. Hart WM Jr. The eyelids. In: Hart WM Jr, editor. Adler's physiology of the eye. St Louis: Mosby-Year Book, 1992:1–17.
3. Mathers WD, Shields WJ, Sachdev MS, Petroll WM, Jester JV. Meibomian gland dysfunction in chronic blepharitis. Cornea 1991;10:277–285.
4. Robin JB, Jester JV, Nobe J, Nicolaides N, Smith RE. In vivo transillumination biomicroscopy and photography of meibomian gland dysfunction. Ophthalmology 1985;92:1423–1426.
5. Shimazaki J, Sakata M, Tsubota K. Ocular surface changes and discomfort in patients with meibomian gland dysfunction. Arch Ophthalmol 1995;113:1266–1270.
6. Jester JV, Rife L, Nii D, Luttrull JK, Wilson L, Smith RE. In vivo biomicroscopy and photography of meibomian glands in a rabbit model meibomian gland dysfunction. Invest Ophthalmol Vis Sci 1982;22:660–667.
7. Chew CK, Jansweijer C, Tiffany JM, Dikstein S, Bron AJ. An instrument for quantifying meibomian lipid on the lid margin: the meibometer. Curr Eye Res 1993;12:247–254.
8. Yokoi N, Mossa F, Tiffany JM, Bron AJ. Assessment of meibomian gland function in dry eye using meibometry. Arch Ophthalmol 1999;117:723–729.
9. Mathers WD, Lane JA. Meibomian gland lipids, evaporation, and tear film stability. Adv Exp Med Biol 1998;438:349–360.
10. Kodama T, Uno T, Hirano N, Yorii H, Ohashi Y. Analysis of normal human meibomian gland lipids. Folia Ophthalmol Jpn 1994;45:223–226.
11. Marx E. Über vitale Färbung des Auges und der AugenliderI. I. Über Anatomie, Physiologie und Pathologie des Augenlidrandes und der Tränenpunkte. Gräfes Archiv f Ophthalmol 1924;114:465–482.
12. Lemp MA. Report of the National Eye Institute/Industry Workshop on clinical trials in dry eyes. CLAO 1995;21:221–232.
13. Norn M. Meibomian orifices and Marx's line: studied by triple vital staining. Acta Ophthalmol 1985;63:698–700.
14. Hykin PG, Bron AJ. Age-related morphological changes in lid margin and meibomian gland anatomy. Cornea 1992;11:334–342.
15. Bron AJ, Benjamin L, Snibson GR. Meibomian gland disease: classification and grading of lid changes. Eye 1991;5:395–411.

Biosketch

Masahiko Yamaguchi, MD, graduated from the Osaka City University School (OCU) of Medicine in 1990, and served as an ophthalmologist at the OCU Hospital from 1990 to 1995. In 1996, he joined the faculty of Ehime University School of Medicine, Department of Ophthalmology, for research on ocular surface diseases. His main area of research is in dry eye.

Changes in Lumen Width of Nasolacrimal Drainage System After Adrenergic and Cholinergic Stimulation

JUNJI NARIOKA, MD, AND YUICHI OHASHI, MD

• PURPOSE: To determine the effect of an adrenergic agonist and a cholinergic agonist on the lumen width of the nasolacrimal drainage system.
• DESIGN: Prospective, nonrandomized, clinical trial.
• METHODS: The asymptomatic sides of 33 patients (23 women, 10 men) with unilateral stenosis/obstruction of the nasolacrimal drainage system were studied. The tear meniscus height of the asymptomatic side was normal, with a patent lacrimal system as reveled by dacryocystography. The nasolacrimal drainage system of the asymptomatic side was infused with 100 μL of 5% phenylephrine hydrochloride (an α-1 adrenoceptor agonist) or 100 μL of 2% pilocarpine hydrochloride (a cholinergic agonist), and dacryocystography was performed to determine the lumen width of the nasolacrimal drainage system.
• RESULTS: Phenylephrine caused a significant increase of the lumen width of the nasolacrimal drainage system, and the changes were more marked in the nasolacrimal duct (NLD), especially the upper and middle regions, than in the lacrimal sac. In contrast, pilocarpine reduced the lumen width of the NLD significantly, especially in the middle and lower regions, and the lumen width of the lacrimal sac was not significantly changed.
• CONCLUSION: The alterations of the lumen width of the nasolacrimal drainage system, especially the lumen width of the NLD by adrenergic and cholinergic agonists, suggest that the lumen width can be changed by the autonomic nervous system. (Am J Ophthalmol 2006; 141:689–698. © 2006 by Elsevier Inc. All rights reserved.)

THE ANATOMIC STRUCTURE OF THE NASOLACRIMAL drainage system (which is made up of the lacrimal canaliculus, nasolacrimal duct (NLD), and lacrimal sac (LS)) has been studied extensively, but only a few investigations have been made on the autonomic innervation to this system.[1,2] Paulsen and associates[2,3] conducted the first detailed immunohistochemical studies on the nasolacrimal drainage system and proposed a new hypothesis on the tear outflow mechanism. They found a wide vascular plexus embedded in the wall of the LS and NLD that is comparable to a cavernous body. This cavernous body-like structure was innervated densely and contained a number of neuropeptides that included substance P, neuropeptide Y, vasoactive intestinal polypeptide, and calcitonin gene-related peptide. The connective tissue and/or blood vessels in this region also were immunopositive for some neuronal markers (which included RT97, S-100 protein, and neuron-specific enolase) and for neuronal enzymes that included tyrosine hydroxylase. On the basis of these findings, Paulsen and associates hypothesized that cholinergic stimulation of the blood vessels in the cavernous body would lead to a swelling of the submucosal cavernous tissue and reduce the diameter of the lacrimal lumen and that adrenergic stimulation would relax the submucosal swelling and improve the tear flow.

The purpose of this study was to determine whether the lumen width of the LS and the NLD is altered by sympathetic and parasympathetic stimulation. Dacryocystography was used to measure the lumen width before and after the stimulations.

PATIENTS AND METHODS

• SUBJECTS: Thirty-three patients (23 women and 10 men; age, 70.8 ± 12.0 years (mean ± SD)) were studied. Because x-rays are used for dacryocystography, we ethically could not use subjects without disease of the nasolacrimal drainage system as control subjects. Instead, we selected patients who had a unilateral stenosis/obstruction of the nasolacrimal drainage system or dacryocystitis with epiphora and mucoid discharge from the medial canthal region. These patients required dacryocystography on the symptomatic side to make a definitive diagnosis and on the asymptomatic side to be certain that the lacrimal drainage system was patent and normal anatomically. All subjects were examined in the Department of Ophthalmology at

Accepted for publication Nov 18, 2005.
From the Department of Ophthalmology, Ehime University School of Medicine, Ehime, Japan (J.N., Y.O.); Department of Ophthalmology, Saijo City Shuso Hospital, Ehime, Japan (J.N.).
Inquiries to Junji Narioka, MD, Department of Ophthalmology, Ehime University School of Medicine, Shitsukawa, Toon, Ehime 791-0295, Japan; e-mail: nariokaj@m2.dion.ne.jp

0002-9394/06/$32.00
doi:10.1016/j.ajo.2005.11.040

Saijo City Shuso Hospital between April and July 2005. Approval for this study was obtained from the Institutional Review Board of the Ehime University School of Medicine. The procedures that were used conformed to the tenets of the Declaration of Helsinki; informed consent was obtained from all subjects after the nature and possible consequences of the study were explained. Patients with any ocular surface diseases, glaucoma, nasal inflammatory diseases, abnormal eyelid position, recent episode of ocular trauma, acute/chronic upper respiratory inflammation, or eye surgery were excluded. Patients with heart disease or bronchial asthma were also excluded because of the possible adverse reaction to the drugs.

The lacrimal drainage system on the asymptomatic side was examined carefully in all patients, and no signs of epiphora and mucoid discharge were recognized. Dacryocystography showed no stenosis/obstruction or dilation of the nasolacrimal system on this side. In addition, the tear meniscus height was normal, and the lacrimal system was patent on nasolacrimal irrigation.

• DACRYOCYSTOGRAPHY: All examinations were conducted by one of the authors (J.N.). Dacryocystography was performed on both sides to compare the differences between the asymptomatic and symptomatic sides to be certain that bilateral anatomic stenosis/obstruction was not present. Dacryocystography was performed with a digital radiographic system (ADR-1000A; Toshiba Medical Systems, Tokyo, Japan), and the images were stored electronically as 1024 × 1024-pixel matrix in a 6-inch image intensifier mode. Under these conditions, one pixel corresponded to approximately 0.118 mm.

To record the x-rays, the patient was placed in a supine position, and both eyes were anesthetized topically with 0.4% oxybuprocaine hydrochloride. Then, 0.5 to 1.0 ml of 61.2% iopamidol (Iopamiron 300; Nihon Schering KK, Osaka, Japan), a water-soluble contrast medium, was infused slowly and steadily under fluoroscopic guidance from the upper punctum into the nasolacrimal drainage system through the canaliculus with a 27-guage lacrimal cannula (outer diameter, 0.4 mm; inner diameter, 0.15 mm; Inami, Tokyo, Japan) that was attached to a 2.5-ml syringe. Because the lumen width can be affected by the pressure of injection, the injections were made with approximately the same low pressure. We injected the contrast medium from the upper canaliculus because the upper canaliculus joins the LS in approximately a straight line; the lower canaliculus is curved[4] and joins the caudal side of the upper canaliculus.[5] In addition, the lower canaliculus is slightly longer than the upper canaliculus.[4,6]

Because the shape of the lumen of the nasolacrimal drainage system is not completely circular but complex with many folds and ridges,[4] dacryocystography was performed from two directions, anteroposterior and oblique (45 degrees lateral oblique). Images were obtained before and after the application of the autonomic drugs. The oblique images were obtained by the rotation of the head approximately 45 degrees to the opposite direction (for example, when the right nasolacrimal drainage system was studied, the head was turned to the left). As a result, both the midsagittal and frontal plane of the patient's head made approximately a 45-degree angle with the radiation beam, although the horizontal plane was almost parallel to the radiation beam.

TABLE 1. Results of Dacryocystography in the Symptomatic Sides

Variable	N (%)
Nasolacrimal stenosis	11 (33.3)
Chronic dacryocystitis caused by nasolacrimal obstruction	9 (27.3)
Functional nasolacrimal obstruction	8 (24.3)
Internal common punctum obstruction	3 (9.1)
Canaliculitis	1 (3.0)
Upper canalicular obstruction + punctal stenosis	1 (3.0)
Total	33 (100)

• EFFECT OF ADRENERGIC AND CHOLINERGIC AGONISTS ON NASOLACRIMAL DRAINAGE SYSTEM: To evaluate the effect of gender, male and female patients were studied separately. Phenylephrine was assigned to the patients whose clinical record ended with an odd number, and pilocarpine was assigned to those patients with an even number. We stopped this study after 10 male patients had been studied, at which point, 23 female patients (12 patients with phenylephrine and 11 patients with pilocarpine) had been studied already.

Group A consisted of 12 women and 5 men with a mean age of 71.4 ± 12.3 years (range, forty-eight to ninety-one years); each patients received 100 μl of 5% phenylephrine hydrochloride, an α-1 adrenoceptor agonist that is used for mydriasis (Neosynesin eye drop solution; Kowa, Tokyo, Japan). Group B consisted of 11 women and 5 men with a mean age of 70.3 ± 11.9 years (range, forty-three to eighty-four years); each patient received 100 μl of 2% pilocarpine hydrochloride, a cholinergic agonist that is used as a topical medication for glaucoma (2% Sanpilo eye drop solution; Santen Pharmaceutical, Osaka, Japan). Both drugs contained chlorobutanol as a preservative agent.

After the control pretreatment dacryocystography images were recorded, approximately 100 μl (which corresponded to 2 or 3 drops) of phenylephrine or pilocarpine was infused into the asymptomatic side from the upper punctum into the nasolacrimal drainage system through the canaliculus with the use of a procedure that is similar to that used to infuse the contrast medium. During the infusion, the lower punctum was compressed to prevent a reflux of the agonists. The patients were asked not to blink and to keep their eyes closed for 15 minutes to reduce the

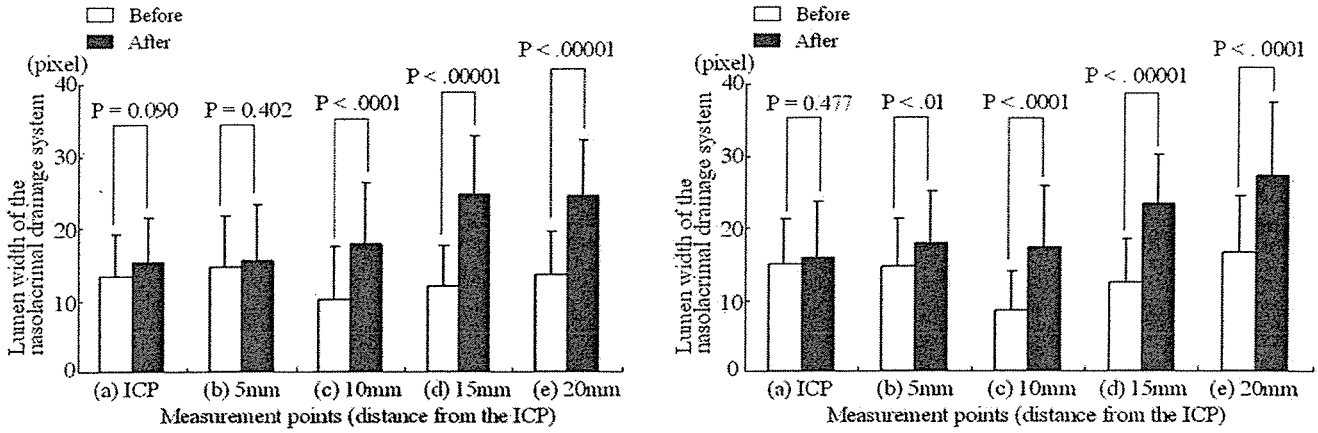

FIGURE 1. Comparison of the lumen width of the nasolacrimal drainage system at five points before and after phenylephrine. The anteroposterior images are shown in Left panel, and the oblique images are shown in Right panel. Analysis was performed with paired *t* tests. (a) = point 1; (b) = point 2; (c) = point 3; (d) = point 4; (e) = point 5; ICP = internal common punctum.

outflow of the drug by lacrimal pumping. Fifteen minutes later, dacryocystography was performed in the anteroposterior and oblique directions to obtain the posttreatment images.

The lumen width of the nasolacrimal drainage system was measured from the dacryocystography images before and after the autonomic agonists. For all measurements, the electronic images were magnified by six times on the basis of the scale required to give 1-cm squares that were nontransparent to radiation. The lumen width was measured by identification of one edge of the duct and the anchoring of one end of an adjustable line at this point. Then the other end of the line was dragged to the other edge of the duct. The length of the line was calculated automatically on the basis of the number of pixels, and the data were displayed. This method is used generally to measure the size of blood vessels in coronary angiograms.[7]

In addition to the absolute size, the ratio of the lumen width before and after drug administration was calculated using the following formula: ratio (%) = $(\alpha - \beta)/\beta \times 100$, where α equals the width after drug administration and β equals the width before drug administration.

It was very difficult to identify the exact borders of the LS, the intraosseous part of the membranous NLD, and the meatal part of the NLD on the dacryocystography. Whitnall[4] reported that the length of the lacrimal sac in cadavers averaged approximately 12 mm and that the distance from the upper end of the LS to the internal common punctum was approximately 2.5 mm. For the NLD, the average length of the intraosseous part of the NLD was 12.4 mm, and the length of the metal part averaged 5.3 mm.[4] Because the vertical axis of the LS and the long axis of the NLD are slightly posterior,[4] the lumen width of the nasolacrimal drainage system was measured at the following five points: point 1 at the level of the internal common punctum, which is approximately the upper LS; point 2, 5 mm below point 1, which is approximately the middle LS; point 3, 10 mm below point 1, which is approximately the lower LS or upper membranous NLD; point 4, 15 mm below point 1, which is approximately the middle membranous NLD; and point 5, 20 mm below point 1, which is approximately the lower membranous NLD.

• STATISTICAL ANALYSES: The Student *t* test was used to compare the values that were obtained from the two groups before drug administration. Paired *t* tests were used to compare the lumen widths before and after the administration at each of the five points, and one-way analysis of variance with a post hoc Tukey test was used for within-group analysis at each measurement point and for analysis of the ratio of the lumen width after drug administration. Repeated-measures analysis of variance were used to compare the drug effects between women and men in each group. A probability value of $<.05$ was taken to be significant. In these calculations, the actual measured pixel-based width was used.

RESULTS

EXCEPT FOR A MILD AND TEMPORARY MYDRIASIS OR MIOSIS that was caused by a reflux of a small amount of the drugs from the punctum, no other complications were seen during the study. After the measurements, there were no complications such as ocular hypertension, nasolacrimal stenosis/obstruction, or dacryocystitis. The results of dacryocystography on the symptomatic side are shown in Table 1.

• DACRYOCYSTOGRAPHY BEFORE AGONISTS: Because the pretreatment lumen widths for the anteroposterior images in group A were not significantly different from that in group B, the values were combined. The mean pretreatment lumen widths that were obtained from the anteroposterior images of the combined group were 1.49 ±

TABLE 2. Comparison of the Lumen Width of the Nasolacrimal Drainage System at Five Points Before and After Phenylephrine (Pixel)

Variable	Anteroposterior Imaging		Oblique Imaging	
	Before	After	Before	After
Internal common punctum	13.4 ± 5.9	15.4 ± 6.1	14.9 ± 6.4	15.8 ± 7.8
5 mm	14.5 ± 7.2	15.4 ± 7.9	14.6 ± 6.6	17.8 ± 7.3*
10 mm	10.2 ± 7.3	17.9 ± 8.3†	8.5 ± 5.5	17.2 ± 8.6†
15 mm	11.8 ± 5.9	24.7 ± 8.0‡	12.5 ± 5.9	23.2 ± 7.0‡
20 mm	13.5 ± 6.1	24.6 ± 7.7‡	16.6 ± 7.6	27.1 ± 10.3†

*$P < .01$.
†$P < .0001$.
‡$P < .00001$.

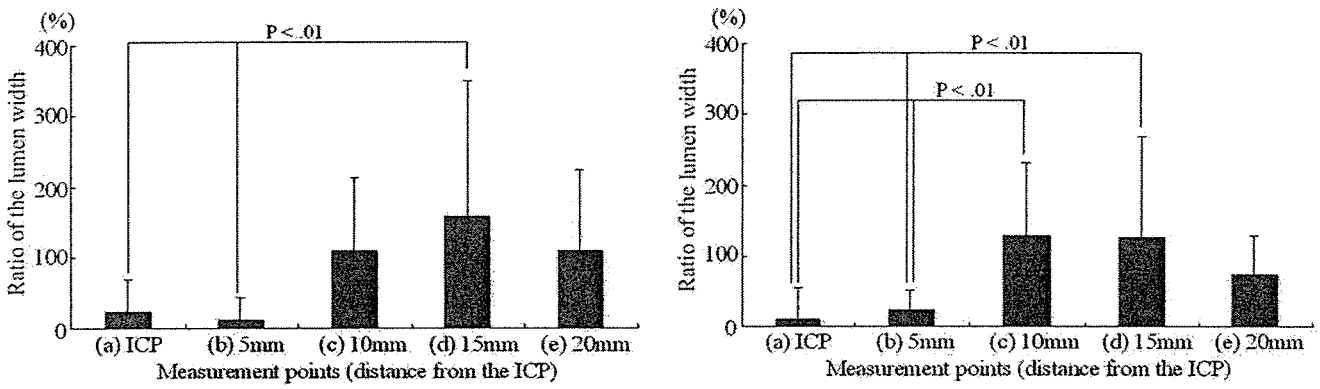

FIGURE 2. Comparison of the change in the ratios of the lumen width after phenylephrine from anteroposterior images (Left panel) and oblique images (Right panel) with the use of one-way analysis of variance with a post hoc Tukey test. (a) = point 1; (b) = point 2; (c) = point 3; (d) = point 4; (e) = point 5; ICP = internal common punctum.

0.6 mm, 1.65 ± 0.7 mm, 1.20 ± 0.8 mm, 1.45 ± 0.7 mm, and 1.77 ± 0.9 mm at points 1 through 5, respectively. The mean pretreatment lumen widths for these same points in the oblique images were 1.71 ± 0.7 mm, 1.86 ± 0.8 mm, 1.07 ± 0.5 mm, 1.42 ± 0.7 mm, and 1.98 ± 1.2 mm, respectively. Most importantly, the lumen widths in the anteroposterior images did not differ significantly from those measured on the oblique images, which would indicate that the nasolacrimal drainage system at these points was approximately circular.

• EFFECTS OF PHENYLEPHRINE AND PILOCARPINE: After phenylephrine infusion, the lumen width was significantly larger than the pretreatment widths at points 3 through 5 in the anteroposterior images (Figure 1, Left panel; Table 2) and at points 2 through 5 in the oblique images (Figure 1, Right panel; Table 2). The lumen widths after drug administration at points 4 and 5 were significantly greater than at points 1 and 2 in the anteroposterior images and at point 5 than at points 1 through 3 in the oblique images. The ratio of the lumen widths before and after drug administration was larger at point 4 than at points 1 and 2 in the anteroposterior images (Figure 2, Left panel) and at points 3 and 4 than at points 1 and 2 in the oblique images (Figure 2, Right panel).

These findings indicate that phenylephrine dilated the lumen width of the nasolacrimal drainage system significantly but that the changes were not uniform along the NLD. Our findings demonstrated that the changes in the lumen width of the NLD were more marked in the upper and middle region of the NLD than in the LS (Figure 3).

In group B, the lumen widths of the nasolacrimal drainage system decreased significantly at points 3 through 5 (Figure 4, Left panel; Table 3); the oblique images showed a significant decrease at points 4 and 5 (Figure 4, Right panel; Table 3). After pilocarpine, the lumen widths at points 3 and 4 were significantly smaller than at points 1 and 2, and the lumen width at point 5 was significantly smaller than that at point 2 in the anteroposterior images. In the oblique images, the lumen widths at points 4 and 5 were significantly smaller than at points 1 and 2, and the lumen width at point 3 was significantly smaller than at point 2. The ratio of the lumen widths showed that the ratios at points 3 through 5 were smaller than at points 1 and 2 in the anteroposterior images (Figure 5, Left panel),

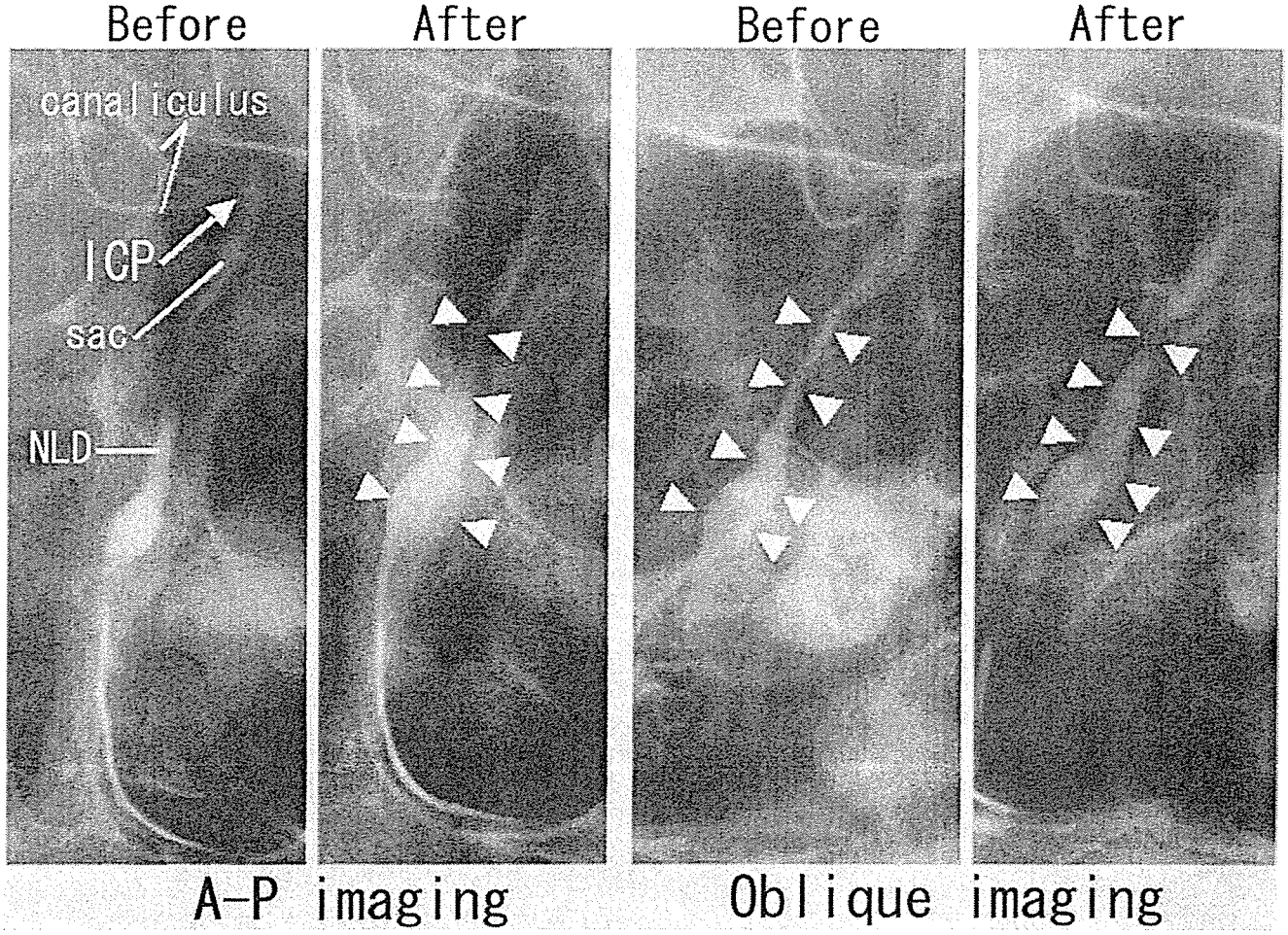

FIGURE 3. Dacryocystography shows dilation of the lumen width of the nasolacrimal drainage system after phenylephrine administration in anteroposterior (A-P) and oblique views (arrowheads), right side. ICP = internal common punctum; NLD = nasolacrimal duct.

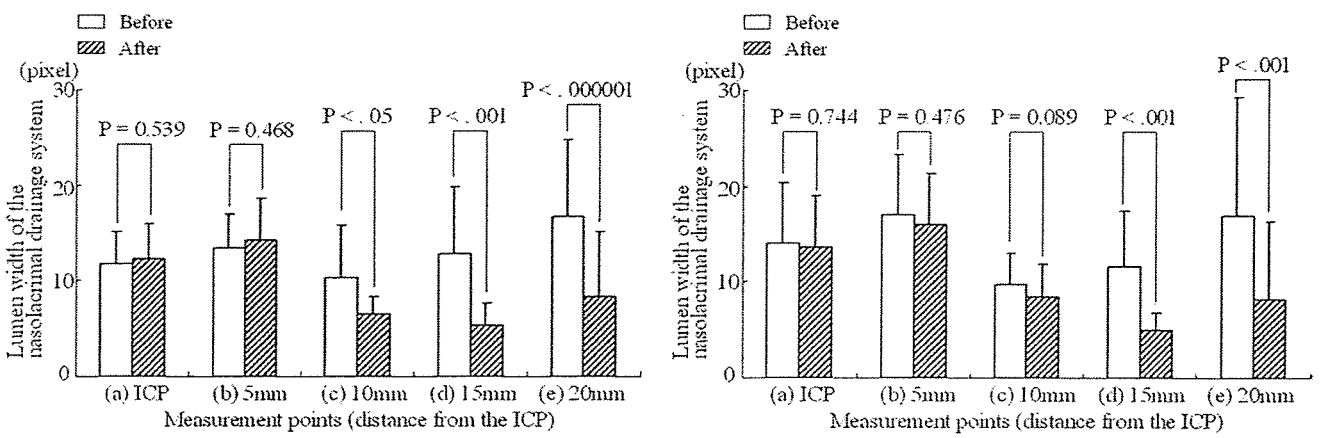

FIGURE 4. Comparison of the lumen width of the nasolacrimal drainage system at five points before and after pilocarpine. The anteroposterior images are shown in Left panel, and the oblique images are shown in Right panel. Analysis was performed with paired *t* tests. (a) = point 1; (b) = point 2; (c) = point 3; (d) = point 4; (e) = point 5; ICP = internal common punctum.

TABLE 3. Comparison of the Lumen Width of the Nasolacrimal Drainage System at Five Points Before and After Pilocarpine (Pixel)

Variable	Anteroposterior Imaging		Oblique Imaging	
	Before	After	Before	After
Internal common punctum	11.8 ± 3.4	12.3 ± 3.7	14.0 ± 6.3	13.7 ± 5.4
5 mm	13.4 ± 3.6	14.3 ± 4.3	17.0 ± 6.4	16.0 ± 5.3
10 mm	10.3 ± 5.6	6.6 ± 1.8*	9.8 ± 3.2	8.5 ± 3.4
15 mm	12.9 ± 7.0	5.4 ± 2.3†	11.6 ± 5.8	5.0 ± 1.8†
20 mm	16.7 ± 8.1	8.3 ± 6.9‡	16.9 ± 12.5	8.2 ± 8.2†

*$P < .05$.
†$P < .001$.
‡$P < .000001$.

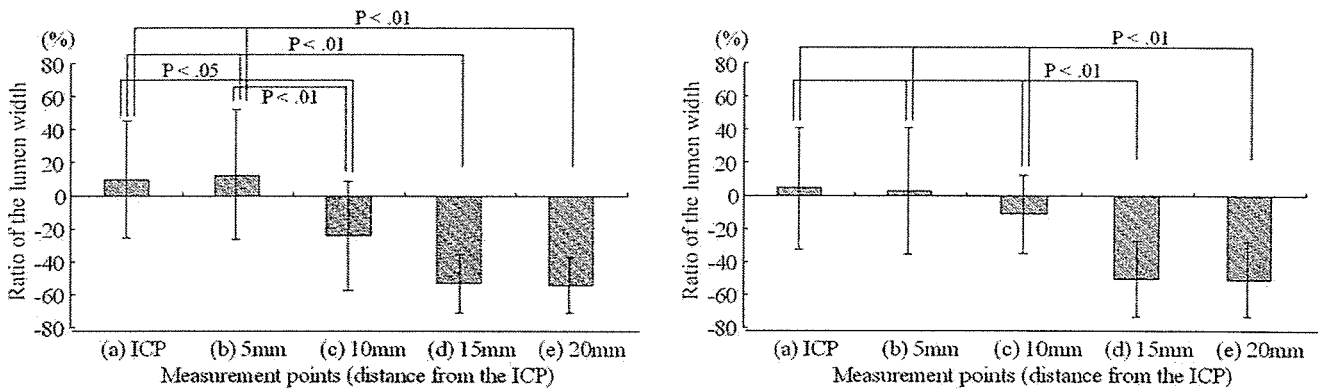

FIGURE 5. Comparison of the change in the ratios of the lumen width after pilocarpine in anteroposterior images (Left panel) and oblique images (Right panel) with the use of one-way analysis of variance with a post hoc Tukey test. (a) = point 1; (b) = point 2; (c) = point 3; (d) = point 4; (e) = point 5; ICP = internal common punctum.

and the ratios at 4 and 5 were smaller than at 1 through 3 in the oblique images (Figure 5, Right panel).

These findings indicate that pilocarpine reduced the lumen width of the NLD significantly and, as with the anteroposterior images, that the changes were not uniform. The changes were more marked in the middle and lower regions, and the lumen width of the LS was unchanged essentially (Figure 6).

• COMPARISON OF DRUG EFFECTS IN WOMEN AND MEN: No significant difference in the degree of change in the lumen width was found between the men and women in either group. These findings indicate that the effects of phenylephrine and pilocarpine are not gender-dependent.

DISCUSSION

OUR RESULTS CLEARLY DEMONSTRATED THAT THE LUMEN width of the NLD is increased by an adrenergic agonist and reduced by a cholinergic agonist. These findings have confirmed the suggestion of Paulsen and associates[2,3] that there is an autonomic network in the NLD. We used 5% phenylephrine and 2% pilocarpine eye drop solutions because these drugs are used widely at these concentrations in daily clinical practice and in general, have no serious adverse reactions. Moreover, this is highest concentration that is available commercially in Japan.

It is well known that the wall of the membranous NLD is thicker than the wall of the LS[4,8,9] and that this cavernous body is well-developed in the NLD and to a lesser extent in the LS. Because the membranous NLD is embedded in the osseous NLD,[4] a change in the lumen width most likely resulted from a change in the thickness of the wall of the membranous NLD rather than a change in the outer diameter. Thus, our observations can be attributed most likely to changes in the cavernous body within the wall of the NLD, and the thick cavernous wall of the NLD may be a key requisite for these changes to occur.

The flow and volume of blood in the nasal mucosa are known to be under autonomic control,[10–13] and there are anastomoses between the dense plexus of the nasal mucosa, the LS, and the NLD.[6] This is significant because the mucosa of the membranous NLD gradually attains the characteristics of the nasal mucosa as it approaches the nasal cavity[4]; thus, the membranous NLD may possess